Inverse Analysis to Estimate Surface Damage Distribution of Thin Panels

Narayanan Ramanujam and Toshio Nakamura
Department of Mechanical Engineering
State University of New York at Stony Brook, Stony Brook, NY 11794

Abstract

When structures are exposed to harsh environmental conditions, their surfaces may be degraded or damaged. Evaluations of these damages on panels and shells often demand complex procedures requiring expensive tools and tedious processes. The aim of this work is development of a method that requires less experimental efforts than those of conventional techniques with an aid of intelligent post-processing scheme. Essentially, this approach utilizes an inverse analysis procedure. First, it constructs approximate functions relating damage conditions to strain field, and then it uses an iterative method to estimate the unknown surface damage distribution. In order to verify its effectiveness, various models are considered and detailed simulation analyses are carried out. Initially, a homogeneous panel with randomly varying damage on an exposed surface is modeled and the accuracy of procedure is evaluated. Following the promising results of homogeneous panel, the scheme is applied to composite laminates with various surface damage/degradation distributions due to matrix erosion. In all cases, excellent agreements are observed between the estimated and exact damage distributions. These results support the present approach as well as similar approaches to be used for reliable damage estimations.

Keywords

Inverse analysis, singular-value decomposition, multivariate Newton's method, damage, degradation, composite panel.

1. INTRODUCTION

Materials in advanced applications such as aerospace structures are designed to possess high strength and specific stiffness. However, they are often exposed to harsh environmental conditions that promote structural aging and exhibit damage/degradation that leads to reduction of their residual strength and remaining life. The lowered damage tolerance may have an adverse effect on structural durability and reliability. Hence, need for detection and quantitative

evaluation of damage arises to prevent catastrophic failures in structures. It is also vital that robust advanced health monitoring systems be developed for the next generation of aeronautical and space systems (Noor et al., 2000).

In many metals, common types of damages occur through surface corrosion, pitting, intergranular corrosion, exfoliation, crevice corrosion, microbial corrosion and filiform (Hagemaier et al., 1985). In general, structural materials are continuously attacked causing corrosion that leads to removal of material not only from the surface but also progressive damage as fresh surfaces of material are exposed. In advanced materials like carbon fiber-reinforced epoxy composites, a different type of material removal may occur. Kumar et al. (2002) observed extensive removal of material due to synergistic degradation mechanisms as shown in Fig. 1. Here a significant amount of epoxy matrix was eroded during repeated exposures to humidity and ultra-violet (UV) radiation. Such a detrimental condition was observed only when the effects of moisture and UV radiation were coupled.

Traditionally, damages are detected using non-destructive evaluation (NDE) techniques such as radiography, ultrasonic, acoustic emissions, electrical, liquid penetration, conductivity, holography, radar and others. Although some are very effective, these procedures often require expensive measurement tools and complex processes to quantify damages. A recent review of NDE techniques by McCann and Forde (2001) noted the high cost for advanced inspection methods such as a radiography method that uses x-ray or γ-ray. It not only requires high capital costs but also large space, high operating costs and long set up time. More importantly, as more complex material/structure systems are being evaluated for damages, it is essential to utilize an *intelligent* approach to process data regardless of measurement techniques.

In the current work, our aim is to develop a method that does not rely on expensive measurement tools but still offers robust damage evaluation. In order to accomplish this goal, an effective approach to process measured record based on an inverse analysis technique is proposed. Recently, various inverse analysis methods have been presented to determine critical parameters in mechanics problems. Maniatty et al. (1989) have utilized an inverse analysis technique coupled with finite element method to solve for elastic and viscoplastic properties of materials. Cao et al. (1998) proposed a different approach based on artificial neural networks for load identification. More recently, Vaddadi et al. (2003) have developed an inverse approach to estimate transient moisture diffusion process in fiber-reinforced composites. Some of the several

investigations to detect damages in structures include a flexibility-based approach for localization and quantification of damages (Bernal and Gunes, 2001), a fiber optic-based method for delamination detection in composites (Leung et al., 2001), remote structural damage monitoring using smart terminals by measuring the frequency response change (Inada et al., 2001), detection of crack by the body force method (Chen and Nisitani, 1993) and damage region identification using neural network-based detectors (Ni et al., 2001).

The present approach involves a post processing of surface strain measurements to identify degradation parameters, which signify the extent of material removal from the surface. Recently, strain sensors/gages are being increasingly used in conjunction with detection of damages in structures (e.g., Fares and Maloof, 1998). However since determination of damage distribution from strains is not directly apparent, we resort to an inverse approach to obtain the best estimates. First, a model, which expresses the strains as functions of the degradation parameters, is developed. Then, the estimation of damage distribution is carried out with multivariate iterative operation. The procedure and its applications are described in detail next.

2. INVERSE ANALYSIS APPROACH

The physical responses of many complex systems can be defined by a set of model/state parameters that are not directly measurable. However, there may be some observable/measurable parameters whose values have functional dependence on the model parameters (Tarantola, 1987). The objective of inverse analysis approach is to determine those unknown state parameters through the measurable parameters. Here, extent of surface degradation is the model/state parameter while surface strains are set as the measurable parameters. Since there are many types of inverse analysis, it is essential to choose a *suitable* technique and set up a *proper* approach for a given problem. Usually, major effort is consumed during choosing an appropriate inverse procedure. During this study, several different approaches were examined, and after several tests, an approach based on a ‘polynomial approximation function’, which accounts for nonlinear effects between the strains and the damage, is adopted. Here, the coefficients in the relations are determined with ‘singular value decomposition’ method. Once the relationship is fully developed, an error minimization problem is formulated and the damage parameters are estimated using ‘multivariate Newton-Raphson method’.

2.1. Damage model

Initially, the proposed inverse scheme is tested with a homogeneous linear elastic plate containing surface damage/degradation. Here, the damage is assumed to occur across one side of the surface that is previously exposed to harsh environment. In order to simulate this condition, a discrete material removal phenomenon is modeled. A comb-like material deletion, as shown in Fig. 2 is assumed to represent the damaged condition. Alternatively, it is possible to vary elastic modulus near the surface to simulate weakening or increased compliance caused by the damages. Such a model would have required less modeling and computational efforts. However, the comb-like model chosen here has more realistic representation of damages observed in actual specimens (e.g., Fig. 1).

In order to quantify the distribution or variation of damage across some length, the panel/beam is virtually divided into sectors as illustrated in Fig. 2. In this study, the damages are assumed to be uniform in the through-thickness direction. The applicability of the present method for damage variations over two-dimensional surface is discussed in Section 5. Here, S is the sector width while t denotes the plate thickness. It is assumed that one axial strain measurement and one averaged damage estimation be made for each sector. For the current approach, an effective range of sector width-thickness ratio is $\sim 2 < S/t < \sim 10$. A smaller ratio would require too many measurements while a larger ratio would not yield precise damage variations. To obtain the influence of damages on the strain, the plate is subjected to pure bending and the axial/longitudinal strain e^{meas} of each sector is measured. Note the present procedure can also accommodate any other types of strain measurements including continuous strain measurements such as by a speckle laser-interferometry or active sensors with radar interferometry (Fares and Maloof, 1998). For large surfaces, these techniques may be more suitable for strain measurements than ones by gages. Various aspects of these measurement procedures are discussed in Section 6.

2.2. Damage-strain relation

Existence of surface damage should influence the deformation behavior of specimen. However the exact nature of damage-strain relationship is very complex and the analytical solution may not exist. Here, a polynomial function is used to obtain an approximate relationship between the strain and the damage. First, the normalized change in strain due to the damage is defined as,

$$D\tilde{e} = \frac{e^{meas} - e_o}{e_o}. \quad (1)$$

Here e_o is a reference strain corresponding to the state of no damage. Next, a dimensionless damage/degradation parameter D is introduced to quantify the extent of average damage within a sector. In this study, the damage parameter D is operationally defined as follows. The parameter is set to range from 0 through 1 with the former value corresponding to no damage and the latter value corresponding to maximum damage. The maximum damage occurs when the average material removal depth (i.e., opening height of comb-like model) in a sector reaches 1/4 of the plate thickness. The parameter scales with the average material removal depth for other cases. This definition is chosen because of its suitability for 4-ply composite laminates considered later. Note, however, any other definitions can be readily accommodated in this approach. With the damage parameter, the strain change is expressed in terms of a series of polynomial terms as,

$$D\tilde{e} = \sum_a a_a D_a + \sum_a \sum_b b_{ab} D_a D_b + \ldots. \quad (2)$$

Here, a_a and b_{ab} are the coefficients that depend on material properties and types of damages and D_a denotes the damage in the sector a. In the above equation, the first summation represents the direct effect while the second double summations express the coupling as well as nonlinear effects of damage in sectors. For thin structures, it is expected that the strain measurement of a sector be influenced by damages of nearby sectors as illustrated in Fig. 2. Obviously, such contribution is greatest from the damage in the same sector (on the opposite side) and it diminishes as the distance increases. Suppose the influence is limited to the three closest sectors, the normalized strain change at sector a can be written as,

$$D\tilde{e}_a = D\tilde{e}(D_{a-1}, D_a, D_{a+1}). \quad (3)$$

The above assumption should be valid as long as $S/t >$ ~2. For a smaller S/t, influences of other neighboring sectors may also have to be considered. In the present formulation, the nonlinear effect due to damage is included up to the second order terms (i.e., quadratic response) and the higher order terms are ignored. With these approaches, the normalized change of strain due to damage (2) can be expanded as,

$$D\tilde{e}_a = c_1 D_a + c_2 (D_a)^2 + c_3 D_{a-1} + c_4 D_a D_{a-1} + c_5 (D_{a-1})^2 + c_6 D_{a+1} + c_7 D_a D_{a+1} + c_8 D_{a-1} D_{a+1} + c_9 (D_{a+1})^2 \quad . \tag{4}$$

Here c's are the unknown coefficients (re-expressed for a's and b's in (2)), which must be determined prior to the inverse analysis. To further simplify the procedure, coupling effects between $D_{a\text{-}1}$ and D_{a+1} are ignored (i.e., $c_8 = 0$) since the corresponding sectors are farther apart. In addition, if widths of all sectors were set equal, it would allow the contribution factors from $D_{a\text{-}1}$ and D_{a+1} to be symmetric (i.e., $c_3 = c_6$, $c_4 = c_7$ and $c_5 = c_9$). With these simplifications, the strain change in terms of damage parameters is,

$$D\tilde{e}_a = c_1 D_a + c_2 (D_a)^2 + c_3 (D_{a-1} + D_{a+1}) + c_4 D_a (D_{a-1} + D_{a+1}) + c_5 [(D_{a-1})^2 + (D_{a+1})^2]. \tag{5}$$

The five coefficients in the above expression are determined with singular value decomposition method as described in Section 2.4.

2.3. Objective Function

In order to extract unknown state parameters, the current inverse analysis minimizes the error between actual strain measurements and strains corresponding to estimated damage distribution. Suppose $D_{a-1}^{est}, D_a^{est}, D_{a+1}^{est}$ are the estimated damage parameters in three neighboring sectors, then corresponding estimated/approximated strain at sector a is expressed as,

$$e_a^{est}(\boldsymbol{D}) = e_o \left[1 + D\tilde{e}_a (D_{a-1}^{est}, D_a^{est}, D_{a+1}^{est})\right]. \tag{6}$$

Here, the objective is to find a damage distribution that yields the minimum error between the *estimated* and *measured* strains across the entire model. The error objective function of sector a can be formulated as,

$$f_a(\boldsymbol{D}) = \frac{e_a^{est}(\boldsymbol{D}) - e_a^{meas}}{e_o} = 1 + D\tilde{e}_a(\boldsymbol{D}) - \frac{e_a^{meas}}{e_o}. \tag{7}$$

Here the vector $\boldsymbol{D}$ contains the unknown damage parameters of all sectors. The minimization of this objective function ultimately leads to the best estimation of damage parameters. The outline of the present inverse analysis procedure is summarized in Fig. 3. The details of singular value decomposition method and multivariate Newton-Raphson method are described next.

2.4. Singular value decomposition

In order to determine the coefficients in (5), the singular value decomposition method (SVD) is utilized. It is an effective technique to diagnose or solve problems involving multiple equations or matrices that are either singular or numerically very close to being singular. It is the method of choice for solving linear least-square problems including parametric data modeling (Press et al., 1992). This method has been also utilized in many problems such as investigation of ill-conditioning of structural identification where small perturbations in experimental data resulted in magnified errors (Hasan and Voila, 1997), optimization of measurement locations for dynamic testing (Penny et al., 1994), and spatial parameter estimation of vibrating structures (Mottershead and Foster, 1991).

To determine the coefficients, values of strains for some damage conditions must be available *a priori*. They can be obtained from model experiments or simulation analyses. In the present analysis, the values are acquired from finite element simulations where various damage distributions are prescribed. Specifically, the calculations are carried out m times, each with different combinations of $D_a{}^i$ and $D_{a\pm1}{}^i$ (where i = 1, 2, … , m), to obtain $D\tilde{e}_a^i$. With (5), the resulting relations between the damages and the strain at a sector can be expressed in a matrix form as,

$$\begin{bmatrix} D_a{}^1 & (D_a{}^1)^2 & 2D_{a\pm1}{}^1 & 2D_a{}^1 D_{a\pm1}{}^1 & 2(D_{a\pm1}{}^1)^2 \\ D_a{}^2 & (D_a{}^2)^2 & 2D_{a\pm1}{}^2 & 2D_a{}^2 D_{a\pm1}{}^2 & 2(D_{a\pm1}{}^2)^2 \\ \vdots & \vdots & \vdots & \vdots & \vdots \\ D_a{}^m & (D_a{}^m)^2 & 2D_{a\pm1}{}^m & 2D_a{}^m D_{a\pm1}{}^m & 2(D_{a\pm1}{}^m)^2 \end{bmatrix} \begin{bmatrix} c_1 \\ c_2 \\ c_3 \\ c_4 \\ c_5 \end{bmatrix} = \begin{bmatrix} D\tilde{e}_a^1 \\ D\tilde{e}_a^2 \\ \vdots \\ D\tilde{e}_a^m \end{bmatrix}. \qquad (8)$$

Suppose the above form to be $\boldsymbol{D}^*\boldsymbol{C} = \boldsymbol{E}$, where $\boldsymbol{D}^*$ is a matrix containing known prescribed damage parameters, $\boldsymbol{C}$ is the unknown coefficient vector and $\boldsymbol{E}$ is the normalized computed strain change. In general, with five unknown components, only five independent equations are sufficient to determine the coefficients. However, since (5) is an approximation relation, the equations in (8) are generally not exact. Here, the aim is to determine $\boldsymbol{C}$ so that good strain approximations can be obtained from given damage conditions. In order to ensure the best fit, $\boldsymbol{C}$ is determined from various combinations of D_a and $D_{a\pm1}$. Their values are varied between 0 and 1 in increments of 0.25 with total of m = 25 combinations. Basically, an over-determined system

of equations is used to minimize the error arising from the polynomial approximation for the strain.

When the matrix is not square, (i.e., $\boldsymbol{D}^*$ is 25×5), it can be decomposed into a column-orthogonal matrix $\boldsymbol{U}$, a square diagonal matrix $\boldsymbol{S}$, and transpose of a square orthogonal matrix $\boldsymbol{V}$ as $\boldsymbol{D}^* = \boldsymbol{USV}^T$. This process is called 'singular decomposition'. Here, five diagonal components of matrix $\boldsymbol{S}$ are the singular values of the matrix that are either positive or zero. Within $\boldsymbol{S}$, the ratio of the largest component over the smallest component is known as the condition number of a matrix. A matrix is *singular* when the condition number is infinite and *ill-conditioned* when its condition number is very large. Once these matrices are computed, the generalized inverse of $\boldsymbol{D}^*$ can be obtained from $\boldsymbol{D}^+ = \boldsymbol{VS}^{-1}\boldsymbol{U}^T$. With this matrix, the coefficient vector is computed as $\boldsymbol{C} = \boldsymbol{D}^+\boldsymbol{E}$. A potential problem with this construction is when one or more of the diagonal components are actually zero. Whenever this happens the reciprocal of the singular values are also set to zero. Doing so ensures that the solution vector gives the exact solution if it exists (Press et. al., 1992). Even when the exact solution does not exist, it gives the closest possible solution in the least squares sense. The generalized inverse matrix $\boldsymbol{D}^+$ in this analysis is obtained with an IMSL subroutine (IMSL, 1999).

2.5. Multivariate Newton-Raphson method

In general, methods for inverse simulations can be divided into techniques that involve numerical differentiation and techniques based upon iterative numerical integration processes. The methods based upon differentiation tend to be at least an order of magnitude faster than those with numerical integrations (Murray-Smith, 2000). The multivariate Newton-Raphson method is a simple but efficient multidimensional root finding method, which falls into the former category. In this approach, the objective is to minimize the error functions in (7). First, the error functions f_a are expanded using Taylor series as,

$$f_a(\boldsymbol{D}+d\boldsymbol{D}) = f_a(\boldsymbol{D}) + \sum_{ß=1}^{n} \frac{\partial f_a}{\partial D_b} dD_b + O(d\boldsymbol{D}^2). \tag{9}$$

A minimization of the error functions $f_a(\boldsymbol{D})$ can be achieved when each component is minimized in the neighborhood of $\boldsymbol{D}$. The higher order terms including $O(d\boldsymbol{D}^2)$ are ignored giving a linear approximation for $f_a(\boldsymbol{D}+d\boldsymbol{D})$. If $f_a(\boldsymbol{D}+d\boldsymbol{D})$ is set to zero, a system of simultaneous linear equations appear as,

$$f_a(\boldsymbol{D}) + J_{ab}\,dD_b = 0 \qquad \text{where} \qquad J_{ab} \equiv \frac{\partial f_a}{\partial D_b}\ . \tag{10}$$

In the above, J_{ab} is a Jacobian matrix and summation over b is assumed. This equation is solved via iterations by adding correction vector $dD_a = -(J_{ab})^{-1} f_b$ to the estimated damage parameters. In general, computations of Jacobian matrix are cumbersome and difficult. However, in the present formulation, the equations are *recursive* and their non-zero components can be explicitly expressed as,

$$\begin{aligned} J_{a(a-1)} &= c_3 + c_4 D_a + 2c_5 D_{a-1}, \\ J_{aa} &= c_1 + 2c_2 D_a + c_4 (D_{a-1} + D_{a+1}), \\ J_{a(a+1)} &= c_3 + c_4 D_a + 2c_5 D_{a+1}. \end{aligned} \tag{11}$$

These components form a banded Jacobian matrix. The inverse of matrix is obtained using the lower triangle-upper triangle (LU) decomposition technique (Press et al., 1992). The iterations are carried out until convergence is obtained. The tolerance is set as $\|f_a(\boldsymbol{D})\| < 1\times10^{-10}$ where $\|f_a(\boldsymbol{D})\|$ is a square norm. Usually it takes about seven increments to converge in the present analysis. The flowchart of the iterative method is illustrated in Fig. 4.

3. DAMAGE DISTRIBUTION OF HOMOGENOUS PLATES

3.1. Model with surface degradation

For initial implementation of the proposed inverse analysis approach, damage evaluation of a homogenous panel is considered. The model is a thin linear elastic plate/beam subjected to four-point bending load, as shown in Fig. 5(a), with Young's modulus E = 200GPa and Poisson's ratio n = 0.3. Here all dimensions are normalized with respect to the plate thickness t. It is assumed that the bottom surface layer is damaged. To determine the distribution of damage, the panel is divided into 16 sectors, denoted as S_1, S_2,…, S_{16}. Here, the sector width-thickness ratio is set as S/t = 5. In each sector, the longitudinal strain is measured on the top surface. Every sector is subjected to a constant bending moment of $10Pt$, where P is the magnitude of applied load.

As described in Section 2.1, damages/degradations are modeled by comb-like geometry representing material removable as illustrated in Fig. 5(b). The finite element mesh of damaged section is shown in Fig. 5(c). A computer code was developed to construct such a model. In the

mesh, smaller elements are placed near the damaged region to resolve higher stresses. The element size increases away from the damaged region. In total, approximately 27,000 generalized plane strain four-noded isoparametric elements are used.

3.2. Determination of strain-damage relations.

Prior to estimating the damage distribution, the coefficients in (5) must be determined for the present model. As no closed-form solution exists, the coefficients for damage-strain relation are obtained by a separate finite element analysis. Since the proposed relation assumes the effect of damage to extend only up to the adjacent sectors, a simplified model is utilized to reduce the modeling and computational efforts. Thus, rather than using the entire model shown in Fig. 5, a smaller model shown in Fig. 6 is considered. Here the longitudinal strain (e_a) at sector a is computed for various values of damage below (D_a) and its adjacent sector ($D_{a\pm1}$). Since symmetric effects are assumed from $D_{a\text{-}1}$ and D_{a+1}, only one half of the plate is modeled. Note that the model assumes a uniform level of damage within each sector. The effects of random and uniform damage distributions within a single sector are discussed in a subsequent section. As discussed earlier, within each sector, the degradation parameter may range from 0 through 1, where 0 indicates no damage and 1 indicates that the damage is at the maximum depth (i.e., equals a quarter of the plate thickness). To choose different combinations, the damage parameters D_a and $D_{a\pm1}$ are both varied from 0 to 1 in increments of 0.25. This means that first $D_{a\pm1}$ is set 0 while D_a is varied from 0 to 1. Next, $D_{a\pm1}$ is set to 0.25 and D_a is again varied from 0 to 1 and so on. In total, 25 separate computations are carried out to obtain various strain values.

Figure 7 shows the effects of damage on the strains under different combinations of D_a and $D_{a\pm1}$. As expected, the axial strain is a strong function of D_a whereas $D_{a\pm1}$ shows a weaker but not negligible effect on the strain. For an example, at $D_a = 0.5$, the change of strain differs by about 24% of the larger value between $D_{a\pm1} = 0$ and 1. With these results, a system of 25 simultaneous equations is formulated; the coefficients in (8) are obtained by solving the singular value decomposition method and listed in Table 1. Here larger values imply larger effects on the strain. As expected, the effects of neighboring damages (c_3, c_5) are smaller than the ones immediately below (c_1, c_2). The coupling effect (c_4) is also only about 8% of the direct effect (c_1).

3.3. Results of damage distributions

In order to examine the validity of the proposed inverse analysis, a *random* distribution of damage/degradation is considered. The levels of damage in various sectors are set by a random number generator. Within each sector, the damage is kept uniform as illustrated in Fig. 8(a). With these damages, the panel is subjected to four-point bend and the surface strains in the sectors, labeled as e_1^{meas}, e_2^{meas}, … e_{16}^{meas}, are obtained from the finite element simulation. The strain measurements in terms of normalized difference across all sectors are shown in Fig. 8(b).

Using these strains as input, the error objective functions (7) are minimized using the multivariate Newton-Raphson method described in Section 2.5. The estimated damage at each sector is shown in Fig. 9. Here the exact/prescribed damage distribution is also noted. The results show the damage estimates to almost match with the exact values at many sectors. Although discrepancies are observed in some sectors, especially with lower damage parameters, they are still within 3% of the maximum damage (i.e., $DD < 0.03$). The high accuracy of these estimates supports the effectiveness of the proposed approach. It is also noted that, in general, the damage estimates of end sectors (i.e., D_1 and D_{16}) may not be as accurate as the others since a strain measurement is available from only one of the adjacent sectors. In the same figure, estimates made by a simple linear relation are included for a reference. Here the damage-strain relation is set to be linear as $D_a = c_o \tilde{De}_a$, where c_o is a constant determined at $D_a = 0.5$ and $D_{a\pm1} = 0.5$ in Fig. 7. This procedure does not require an inverse method but the maximum error in this case is as much as 15% of the maximum damage. The results should justify the importance of including the second order and coupling terms too in the damage estimate approach.

3.4. Effects of sector width

The accuracy of estimates can be influenced by the sector width (with respect to the thickness). For example, if the sector width-thickness ratio is very high (e.g., $S / t > 10$), there should be no coupling effects from damages at the neighboring sectors. On the contrary, if a smaller sector width-thickness ratio were chosen, the coupling effects may be more significant. In order to evaluate the present procedure with larger coupling effects, simulations are carried out with a reduced sector width ($S / t = 2.5$). First, various calculations with different combinations of D_a and $D_{a\pm1}$ are carried out to determine the coefficients in (5). Computed normalized strain changes for various values of damage parameters are shown in Fig. 10. These

results are used in the singular value decomposition method to obtain the coefficients, as listed in Table 1. In this model, greater effects of the adjacent sector (i.e., higher c_3 and c_5) as well as stronger coupling effect (i.e., higher c_4) can be observed.

In the simulation of full model under bending, damages are again distributed randomly. The damaged model is shown in Fig. 11(a). Here the sector width is halved and the total number of sectors is doubled to 32. With e_1^{meas}, e_2^{meas}, … e_{32}^{meas} as inputs, the multivariate Newton-Raphson iterations are carried out to estimate damages in sectors and obtained as shown in Fig. 11(b). In each sector, agreement between the exact and estimated damage parameter is excellent. These results confirm the effectiveness of present approach even with a smaller sector width-thickness ratio. Though not examined in detail, the present approach should produce accurate estimates for models with even smaller sector widths when damage distribution is reasonably smooth across the surface (i.e., unlike the random model shown here). Although models with smaller sector widths yield more detailed estimates of damage variation, they also require more strain measurements. In those cases, a full-field type measurement may be more appropriate for the strain input.

4. DAMAGE DISTRIBUTION OF COMPOSITE PLATES

4.1. Model with surface degradation

The proposed inverse analysis approach is extended to composite laminates with degradation. As noted earlier, when carbon fiber-reinforced composites were exposed to multiple environmental conditions, extensive removal of matrix materials had occurred (Kumar et al., 2002). In such a condition, quantification of degradation/damage is essential for predicting residual strength and long-term durability of composites. In this analysis, simulations are carried out with two models with 4-ply $[90/0]_s$ and 8-ply $[90/0]_{2s}$ arrangements. In each ply, the material is assumed to be transversely isotropic, and their linear anisotropic properties are E_L = 125GPa, E_T = 8.50GPa, ν_{LT} = 0.330, ν_T = 0.176 and G_{LT} = 56.4GPa, where, the subscript '*L*' indicates the fiber direction while the subscript '*T*' indicates the transverse direction. These properties are representative of IM7/997 carbon-fiber/epoxy composite supplied by Cytec-Fiberite, Inc.

The schematic in Fig. 12(a) represents the composite laminate subjected to remote bending with damages in the bottom layer and proposed strain measurements on the top surface. An enlarged section of the lower plies are shown in Fig. 12(b). The $[90/0]_s$ laminate shown here has

a symmetric arrangement of plies. The 0° ply has the fibers along the axial/longitudinal direction while the 90° ply has the fibers oriented along the out-of-plane direction. A comb-like damage model is again utilized to simulate the material removal due to the environmental effects. Here damages are assumed to be within the bottom ply since the next ply has 0° fiber arrangement (i.e., along the axial direction) and any matrix erosion in this ply would have negligible effect on the overall deformation (i.e., fibers carry most of the load). In fact this is the reason why $[90/0]_s$ arrangement is chosen and not $[0/90]_s$; to maximize the deformation due to damage. In order to simulate, a finite element mesh similar to that of the homogeneous model is constructed. A generalized plane strain condition is again assumed.

4.2. Damage distribution of 4-ply $[90/0]_s$ laminate

First, the reference damage-strain relation for the composite panel is determined using a model similar to the one shown in Fig. 6. As in the case of homogeneous panel, D_a and $D_{a\pm1}$ are both varied from 0 to 1 in increments of 0.25, and 25 computations are carried out to determine the coefficients in (5). The coefficients obtained via the singular value decomposition method are listed in Table 1.

Two different distributions of degradation are considered for the composite panel. For the first case, damages are distributed randomly as in the case of homogenous model. The damaged model is shown in Fig. 13(a). Here, the sector width-thickness ratio is again set as $S/t = 5$. A finite element simulation is carried out for this model and longitudinal strains on the top surface are computed. Using the computed strains as input, the multivariate Newton-Raphson method is performed to estimate the damage distribution. Figure 13(b) shows the estimated damage in each sector as well as the exact/prescribed damage. Again in this case, agreements are excellent across various sectors and the results support the effectiveness of the current approach to predict damage distribution.

Under ordinary conditions, if panels were exposed to a harsh environmental condition, one would expect to observe more continuous or smooth degradation distributions across the surfaces. So instead of using another discontinuous damage model as the previous case, a damage model with sinusoidal distribution is considered next as shown in Fig. 14(a). The period of sinusoidal curve is set slightly longer than the total length of sectors and the maximum damage amplitude is set at $D = 0.94$. Furthermore, to make the damage condition more realistic,

damages are varied randomly in the range of DD = 0.06 within each sector. The model is subjected to bending and the surface strains are computed. The strains are used as input to the multivariate Newton-Raphson method and estimates of damages are made. Figure 14(b) shows the exact as well as the estimated damage distribution. Note since the model geometry and properties are identical to those of previous random model (other than the damages), the same coefficients obtained in the previous analysis can be used here. Again the results show the estimates to be very close to the exact/prescribed damages. They also suggest the effect of local random damages within a sector to be small, and they appear to be no different from the model with uniform damage within a sector.

4.3. 8-ply $[90/0]_{2s}$ laminate

To study the applicability of the current approach for laminates with higher number of plies, 8-ply $[90/0]_{2s}$ laminate is considered next. Here each ply is half as thick as the previous 4-ply model, and the maximum possible damage is also reduced by half. Prior to the estimation of damages, the coefficients in damage-strain relation (5) must be determined again. Using a similar model as the previous ones, the variations of the axial strain are determined as functions of D_a and $D_{a\pm1}$. Here D_a and $D_{a\pm1}$ are both varied from 0 to 0.5 in increments of 0.125. The computed coefficients via SVD method are listed in Table 1. With an increased number of plies in the model, it shows decreased damage effects on the strains. Here the maximum change in the strain due to presence of damages is only about 4% of undamaged case, as opposed to about 17% for the 4-ply model. Furthermore, the nonlinear and coupling effects are also smaller for this model. These results suggest a more difficult estimation process.

Full model simulations are carried out to obtain strains of damaged panel. Here a slightly more refined mesh with approximately 29,000 elements is constructed since the damage is confined to a smaller region. Although several damage cases are examined, only the results of a sinusoidal variation of damages (similar to the second case of the 4-ply model) are presented. The damages are prescribed to follow the sinusoidal distribution with the maximum damage set as D = 0.47. As shown in Fig. 15(a), the damage within a sector is set to vary randomly. The panel is subjected to four-point bending and its surface strains are computed. The strains are used in the multivariate Newton-Raphson method and the estimated damages are obtained as shown in

Fig. 15(b). Despite the smaller effect of damages on the strains, a remarkable agreement between the actual and estimated damages is obtained.

5. EXTENSION TO THREE DIMENSIONAL MODELS

Even though the current study assumed the damages to be uniform in the thickness direction, this approach can be readily extended to models with damage variations in two directions. In such cases, damage distributions must be determined not only along the longitudinal direction but also the through-thickness direction. Thus the panel would be divided into virtual sectors/sections over two-dimensional surface. The average damage at one section then can be expressed as $D_{a,b}$, where a and b denote the sector numbers along the longitudinal and thickness directions, respectively. In this section, the procedure to extend the current method to full three-dimensional models is briefly described.

5.1. Damage-Strain Relation

Using the similar assumptions applied in (5), the damage-strain relations for full three-dimensional model can be extended as,

$$\begin{aligned} D\tilde{e}_{a,b} = {} & c_1 D_{a,b} + c_2 D_{a,b}^2 + 2c_3 D_{a\pm1,b} + 2c_4 D_{a,b} D_{a\pm1,b} + 2c_5 D_{a,b\pm1} + 2c_6 D_{a,b} D_{a,b\pm1} \\ & + 4c_7 D_{a\pm1,b\pm1} + 4c_8 D_{a,b} D_{a\pm1,b\pm1} + 2c_9 D_{a\pm1,b}^2 + 2c_{10} D_{a,b\pm1}^2 + 4c_{11} D_{a\pm1,b\pm1}^2 \end{aligned} . \quad (12)$$

Here, $2D_{a\pm1,b}$ implies ($D_{a+1,b}$ + $D_{a-1,b}$) and others with '±' have similar implications. Also the damage parameters $D_{a+1,b}$ and $D_{a-1,b}$ are set to have equivalent effects and so are the parameters $D_{a,b+1}$ and $D_{a,b-1}$. The above formula requires determination of eleven independent coefficients, which can be difficult to determine accurately. The number of coefficients can be reduced in the following manner. Suppose the coupling effects from the *diagonally adjacent* sections are small, then one can set $c_8 = 0$. Furthermore, if the nonlinear effects of adjacent sectors are ignored, then one can also set $c_9 = c_{10} = c_{11} = 0$. These simplifications lead the relation to be expressed as,

$$\begin{aligned} D\tilde{e}_{a,b} = {} & c_1 D_{a,b} + c_2 D_{a,b}^2 + 2c_3 D_{a\pm1,b} + 2c_4 D_{a,b} D_{a\pm1,b} + 2c_5 D_{a,b\pm1} \\ & + 2c_6 D_{a,b} D_{a,b\pm1} + 4c_7 D_{a\pm1,b\pm1} \end{aligned} . \quad (13)$$

The above strain-damage relation reduces the total number of coefficients to seven, which is a more manageable number. Based on the two-dimensional models, the elimination of nonlinear

terms in adjacent sectors can result in as much as 4% error (for $S/t = 5$). Although a similar error is possible for the three-dimensional model, actual error may be smaller since damages from more sectors contribute in defining the strain.

5.2. Objective Function

In order to estimate the unknown damage parameters, it is necessary to formulate an objective function or the error function in terms of the measured and estimated strains. The estimated strain can be written as,

$$e_{a,b}^{est} = e_{\mathrm{o}} \left[1 + D\tilde{e}_{a,b}(D_{a,b}, D_{a\pm1,b}, D_{a,b\pm1}, D_{a\pm1,b\pm1})\right]. \tag{14}$$

The objective functions for the three-dimensional case can be expressed in a matrix component form as,

$$f_{a,b}(\boldsymbol{D}) = \frac{e_{a,b}^{est}(\boldsymbol{D}) - e_{a,b}^{meas}}{e_{\mathrm{o}}}. \tag{15}$$

Here $f_{a,b}(\boldsymbol{D})$ is the local error function of section (a,b). Also the *matrix* $\boldsymbol{D}$ contains the unknown degradation parameter of every section. As in the previous cases, e_{o} represents the reference strain corresponding to the state of no damage. The above matrix function can be minimized to obtain the best estimates of damage distributions across the surface using the multivariate Newton-Raphson method.

6. DISCUSSIONS

A novel approach based on an inverse analysis is introduced to estimate damage and degradation distribution on a panel surface. The scheme is explored as an alternative to traditional damage evaluation techniques, which generally require high set-up costs and complex measurement procedures. This inverse approach processes strain measurements to extract best estimates of damage fields. The present verification study based on simulations supports the effectiveness of the technique. Although this study considered two-dimensional geometry, the approach can be readily extended to three-dimensional models as described in Section 5.

The key features of this approach and the main observations of our study can be summarized as below.

1. An effective damage-strain relation that considers nonlinear as well as coupling effects is developed. The accuracy of this relation is vital to the inverse approach to estimate the unknown parameters.
2. The inverse analysis methodology also utilizes the powerful singular decomposition technique to determine the coefficients in the damage-strain relation. This technique ensures the existence of solutions even for numerically singular problems (e.g., even when the strains are very weak functions of the damage/degradation).
3. To determine the multiple unknowns (i.e., damages at multiple sectors), the multivariate Newton-Raphson method is utilized, which is an efficient root finding iterative method. One potential problem with this method is that it could fail if convergence to the exact solution is unstable. If it occurs, one may need to use a modified form of the Newton-Raphson method or resort to multi-dimensional descent techniques for minimization.
4. The present method is applied to homogenous and composite panel with one surface with damages. The results show excellent match between the actual/prescribed damages and the estimated damages via surface strains.

We also note that procedure can be extended to three-dimensional models as described in Section 5. As in the two-dimensional models, the current method should be effective when sector/section lengths are chosen as 2~5 times the plate thickness. This method can easily accommodate full-field strain measurements as the input to damage estimation. Such measurements may be more suitable for three-dimensional models.

Although the effectiveness of the approach is presented through the detailed simulation study here, implementation of this method in actual experiments should require further considerations. First, measurement errors must be accounted. Any errors in strain measurements can translate to inaccurate estimation of damage distribution. Second, if computational models are used to define reference strain-damage relations as done here, then they should represent the nature of damage well. The comb-like model adopted here may not be suitable for certain damage mechanisms that cause very localized but extensive damage. Third, detections of strain changes due to damages may be difficult in some panels, especially when composite laminates with many plies (e.g., 32, 64 plies) are considered. In those cases, strain measurements on the opposite side of damaged surface are not appropriate. Since measurements directly on the damaged surface are not practical either, an alternate type of strain measurements would be necessary. For an example,

embedded strain sensors with optical fibers may detect the strain changes more precisely. Obviously such a technique is not only more costly but it must be designed prior to panel manufacturing process. In fact, embedded sensor panels are increasingly being considered for health monitoring of structures. Even in those systems, the principal of current procedure is still applicable. Similar models can be still used to process measured strains and then obtain best estimates of damages. Furthermore, the current approach can be also modified to accommodate measurements other than strains (e.g., electrical current) to estimate damages.

Acknowledgements

The authors gratefully acknowledge the U.S. Army Research Office for their support under DAAD19-02-1-0333. The computations were carried out using finite element code ABAQUS, which was made available under academic license from Hibbitt, Karlsson and Sorensen, Inc.

References

Bernal, D., Gunes., B., 2001. A Flexibility-Based Approach for the Localization and Quantification of Damage: Application in a Benchmark Structure. Structural Health Monitoring: The Demands and Challenges, CRC Press, Florida.

Cao, X., Sugiyama, Y., Mitsui, Y., 1998. Application of artificial neural networks to load identification. Computers and structures 69(1), 63-78.

Chen, D.H., Nisitani, H., 1993. Detection of a crack by body force method. Engineering Fracture Mechanics 45(5), 671-685.

Fares, N., Maloof, R., 1998. Crack detection characterization of strain sensing grids. International Journal of Solids and Structures 35(22), 2861-2875.

Hagemaier, D.J., Wendelbo, Jr., A.H., Bar-Cohen., Y., 1985. Aircraft corrosion and detection methods. Materials Evaluation 43(4), 426-437.

Hasan, W.M., Voila, E., 1997. Use of the singular value decomposition method to detect ill-conditioning of structural identification problems. Computers and Structures 63(2), 267-275.

IMSL Mathematical and Statistical Libraries, 1999. Visual Numerics, Inc., San Ramon, California.

Inada, T., Todoroki, A., Sugiya, T., 2001. Remote structural monitoring via internet with frequency response change method. Structural Health Monitoring: The Demands and Challenges, CRC Press, Florida.

Kumar,B.G., Singh.,R.P., Nakamura.,T., 2002. Degradation of carbon fiber-reinforced epoxy composites by ultraviolet radiation and condensation. Journal of Composite Materials 36(24), 2713-2733.

Leung, C.K.Y., Yang, Z., Xu, Y., Tong, P., Lee, S.K.L., 2001. A new fiber optic-based method for delamination detection in composites. Structural Health Monitoring: The Demands and Challenges, CRC Press, Florida.

Maniatty, A., Zabaras, N., Stelson, K., 1989. Finite element analysis of some inverse elasticity problems. Journal of Engineering Mechanics 115(6), 1303-1317.

Maniatty, A., Zabaras, N., 1989. Method for solving inverse elastoviscoplastic problems. Journal of Engineering Mechanics 115(10), 2216-2231.

McCann, D.M., Forde, M.C., 2001. Review of NDT methods in the assessment of concrete and masonry structures. NDT & E International 34(2), 71-84.

Mottershead, J.E., Foster, C.D., 1991. On the treatment of ill-conditioning in spatial parameter estimation from measured vibration data. Mechanical Systems and Signal Processing 5(2), 139-154.

Murray-Smith, D.J., 2000. The inverse simulation approach: a focused review of methods and applications. Mathematics and Computers in Simulation 53(4-6)**,** 239-247.

Ni, Y.Q., Ko, J.M., Zhou, X.T., 2001. Damage region identification of cable-supported bridges using neural network based novelty detectors. Structural Health Monitoring: The Demands and Challenges, CRC Press, Florida.

Noor, A.K., Venneri, S.L., Paul, D.B., Hopkins, M.A., 2000. Structures Technology for Future Aerospace Systems. Computers and Structures 74(5), 507-519.

Penny, J.E.T., Friswell, M.I., Garvey, S.D., 1994. Automatic choice of measurement locations for dynamic tests. AIAA Journal 32(2), 407-414.

Press, W.H., Teukolsky S.A., Vetterling W.T., Flannery, B.P., 1992. Numerical Recipes in C: The Art of Scientific Computing, Cambridge University Press, United Kingdom.

Tarantola, A., Inverse Problem Theory: methods for data fitting and model parameter estimation, 1987. Elsevier Inc., New York.

Vaddadi, P., Nakamura, T., Singh, R.P., 2003. Inverse analysis for transient moisture diffusion through fiber-reinforced composites. Acta Materialia 51(1), 177-193.

Models	Coefficients (%)				
	c_1	c_2	c_3	c_4	c_5
Homogenous (S/t = 5)	35.7	29.1	2.56	–2.99	2.95
Homogenous (S/t = 2.5)	31.9	28.8	4.62	–5.47	5.42
Composite - 4-ply (S/t = 5)	21.3	–5.84	1.61	–0.900	–0.129
Composite - 8-ply (S/t = 5)	4.63	–0.795	0.305	–0. 095	–0.005

Table 1. Coefficients of nonlinear equations defining relationships between strain and damage parameters for different models.

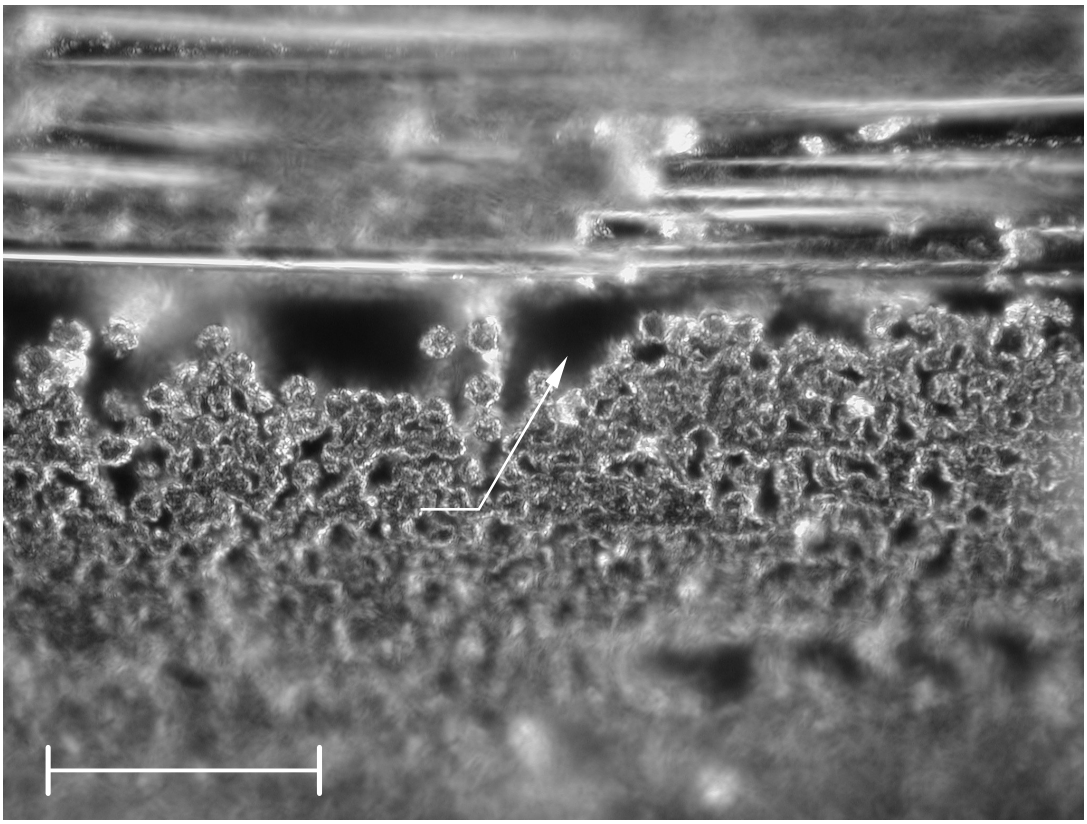

Fig. 1. Optical micrograph of degraded carbon fiber-reinforced epoxy matrix near interlaminar interface exposed to 1,000 hours of repeated moisture and UV radiation.

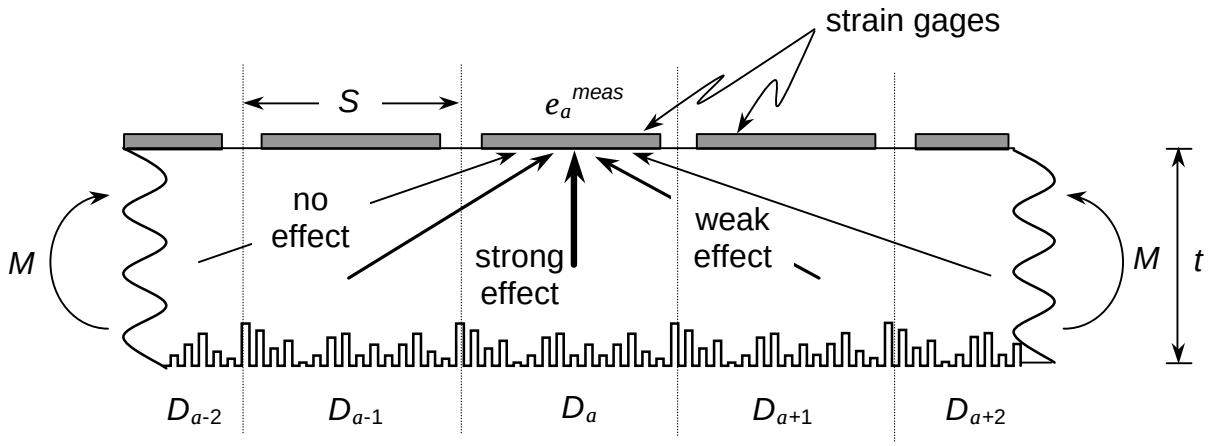

Fig. 2. Schematic of surface damaged plate represented by comb-like material removal. Strain measurement is made on the opposite surface under remote bending at each sector. Effects of damages at neighboring sectors are also illustrated.

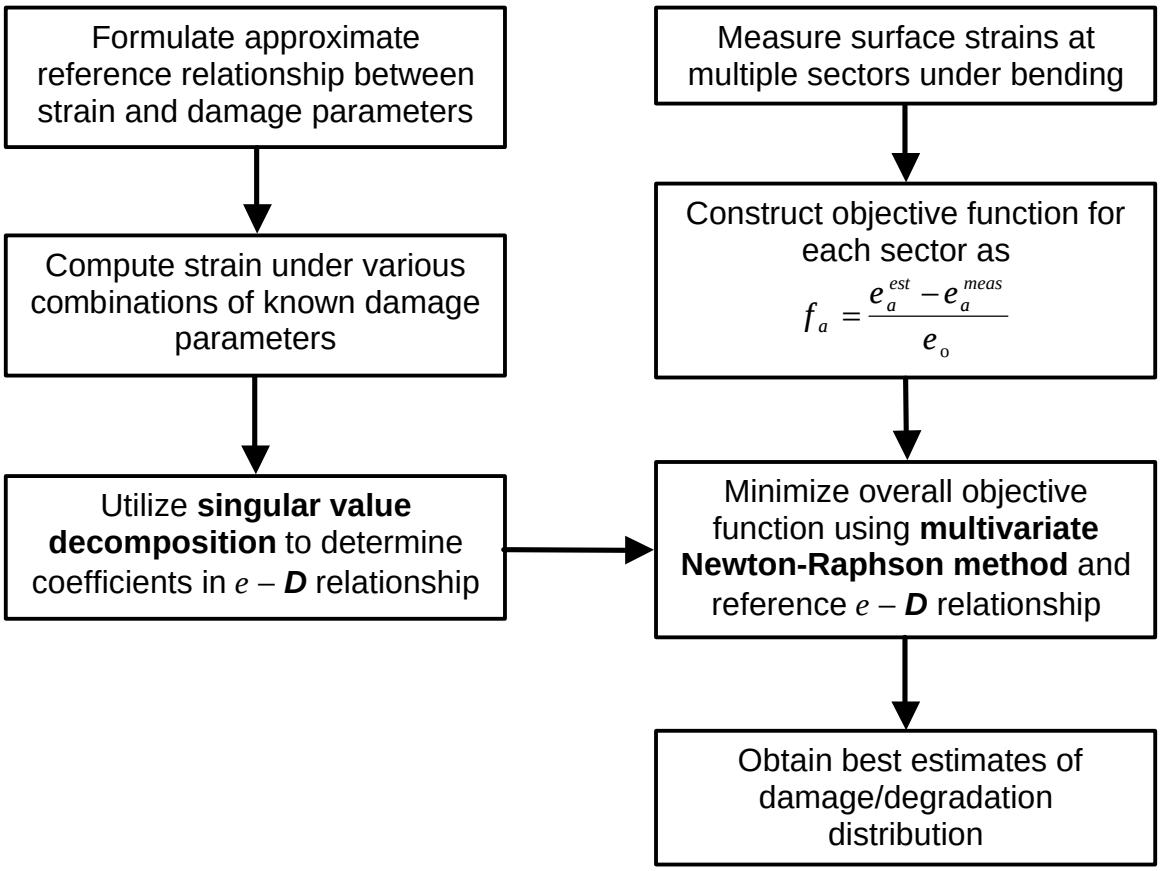

Fig. 3. Outline of the inverse analysis procedure to estimate damage distribution.

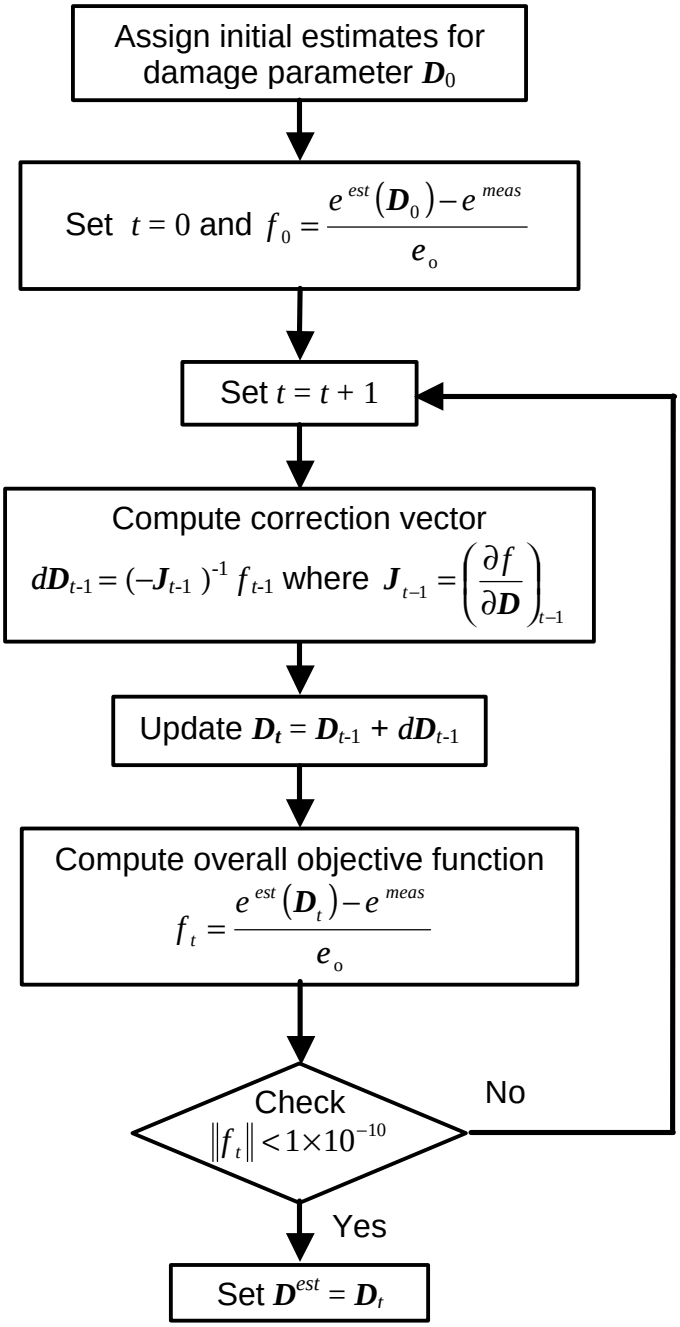

Fig. 4. Flowchart for multivariate Newton-Raphson method.

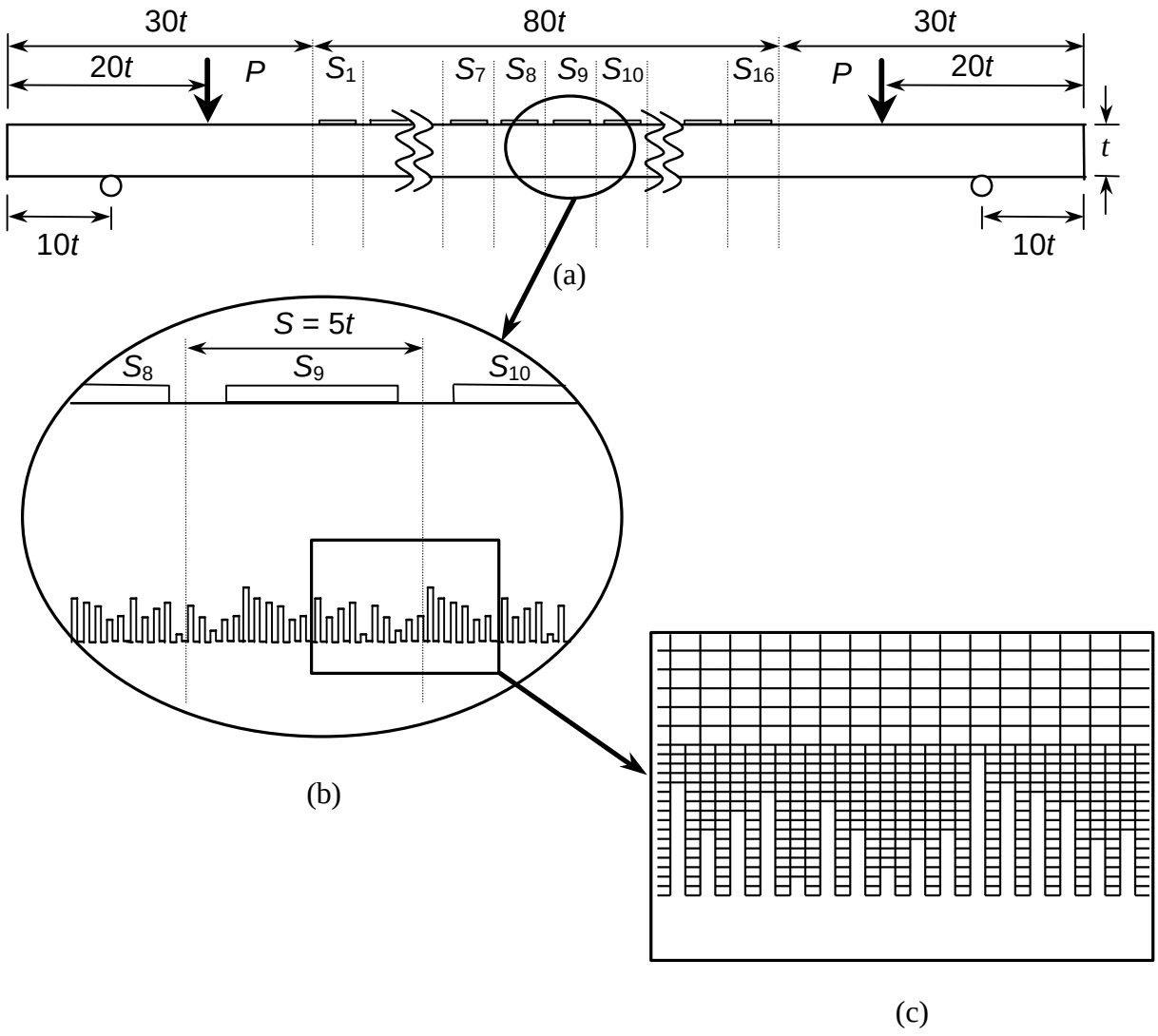

Fig. 5. (a) Surface damaged homogenous plate model subjected to four-point-bend. (b) Enlarged section of model showing comb-like degradation on exposed surface. (c) Finite element mesh near damage. Vertical dimensions are magnified by 5 times in (a), (b) and (c).

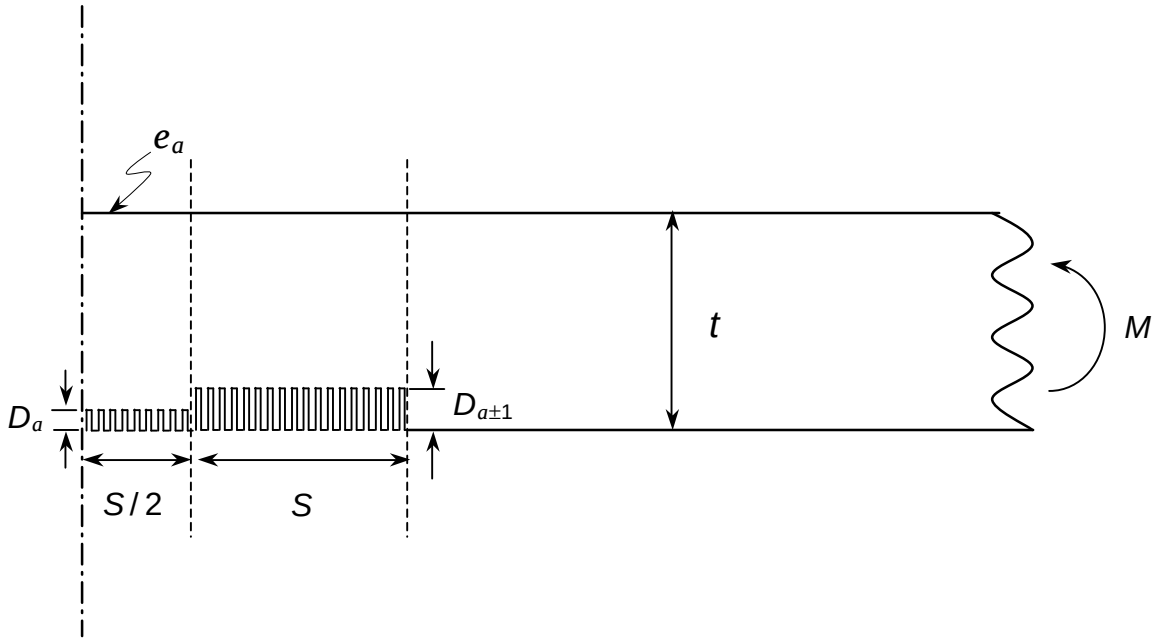

Fig. 6. Schematic of model used to determine unknown coefficients relating damage to strain under remote bending. Vertical dimensions are magnified by 5 times for clarity.

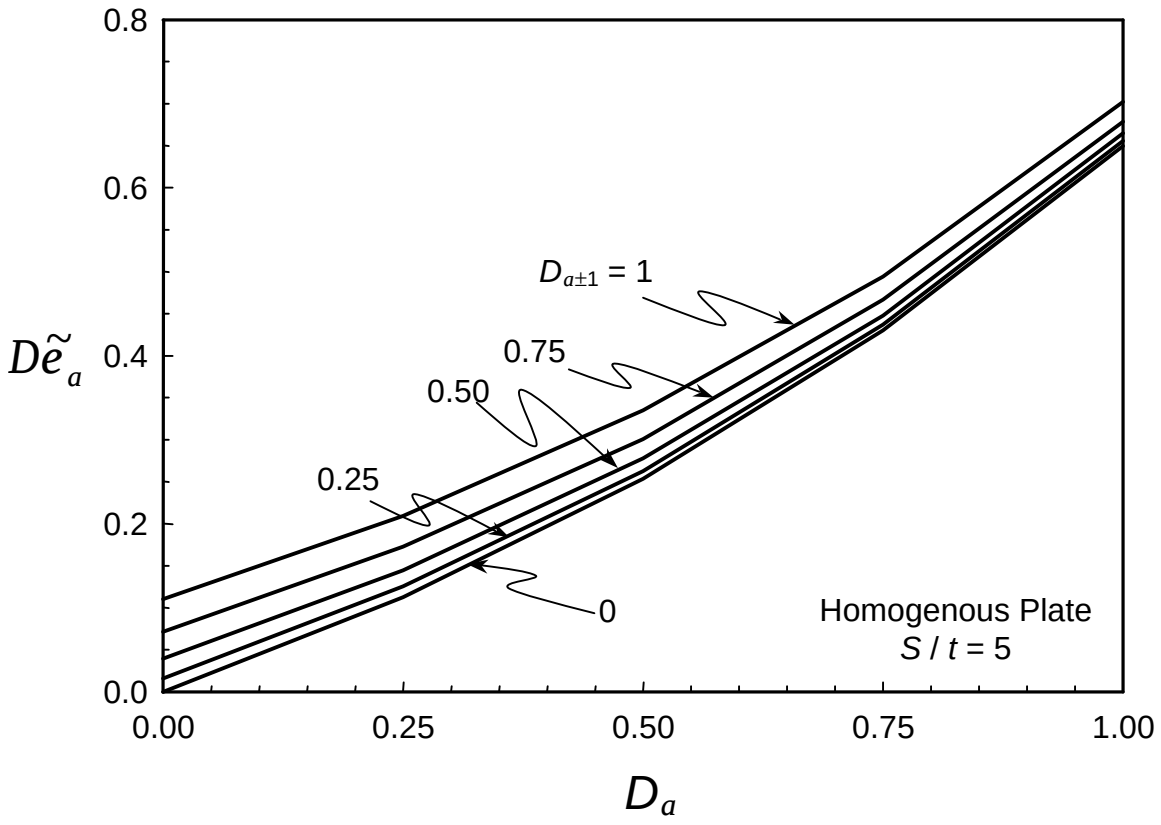

Fig. 7. Effect of damage on strain measurement in sector a is shown for different combinations of D_a and $D_{a\pm1}$ (homogeneous plate with S / t = 5).

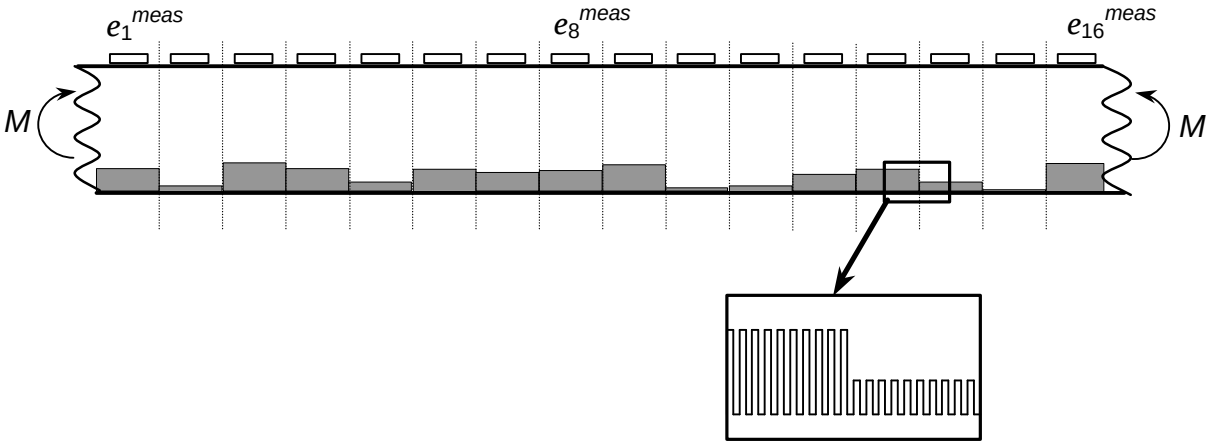

(a)

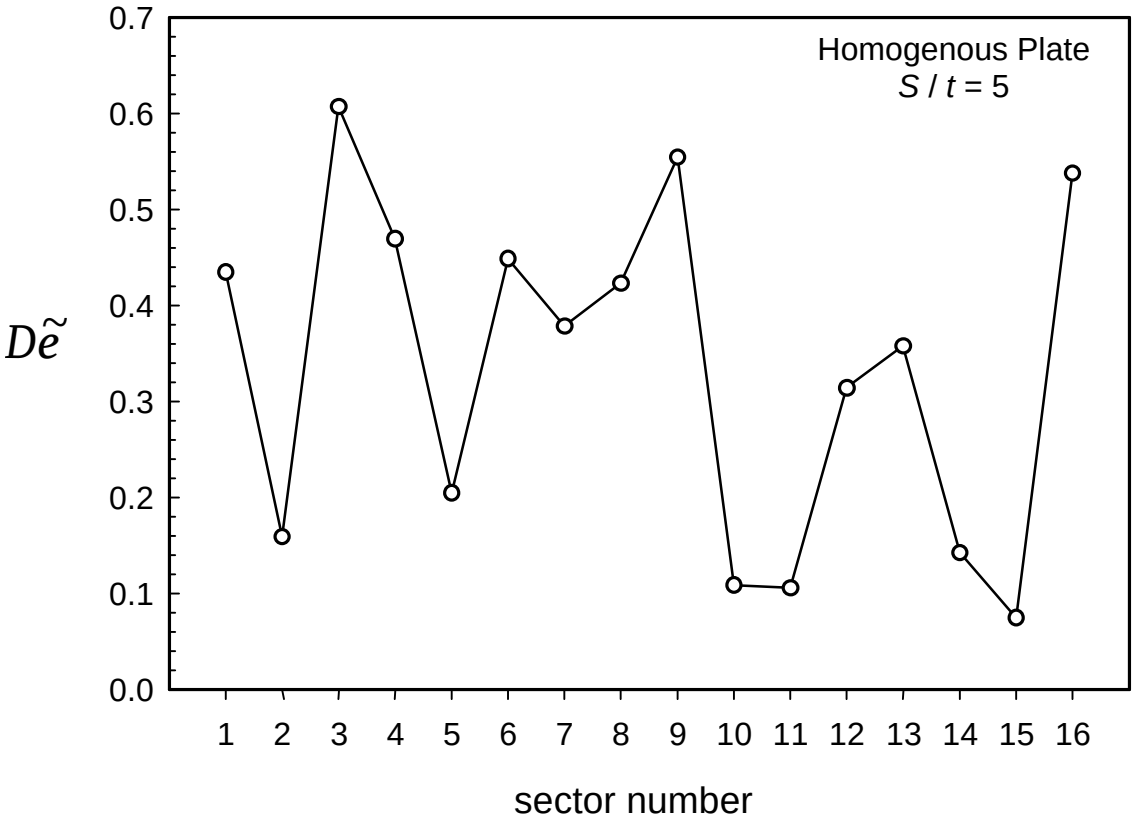

(b)

Fig. 8. (a) Homogenous plate subjected to bending with randomly varied damage in different sectors (constant within a sector). Vertical dimensions are magnified by 10 times for clarity. (b) Corresponding strain measurements (in terms of normalized difference) across all sectors.

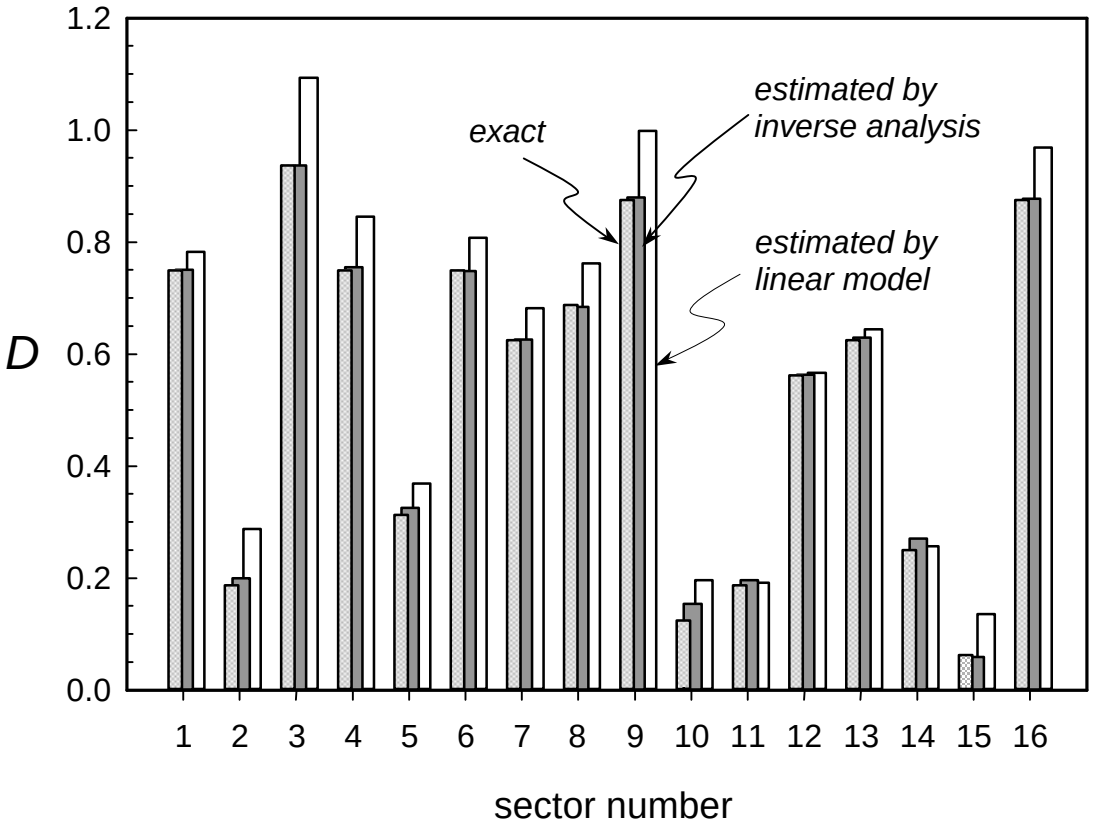

Fig. 9. Distributions of exact/prescribed damage and estimated damage across sectors for homogenous plate (S / t = 5). Estimates by a simple linear model are also shown for reference.

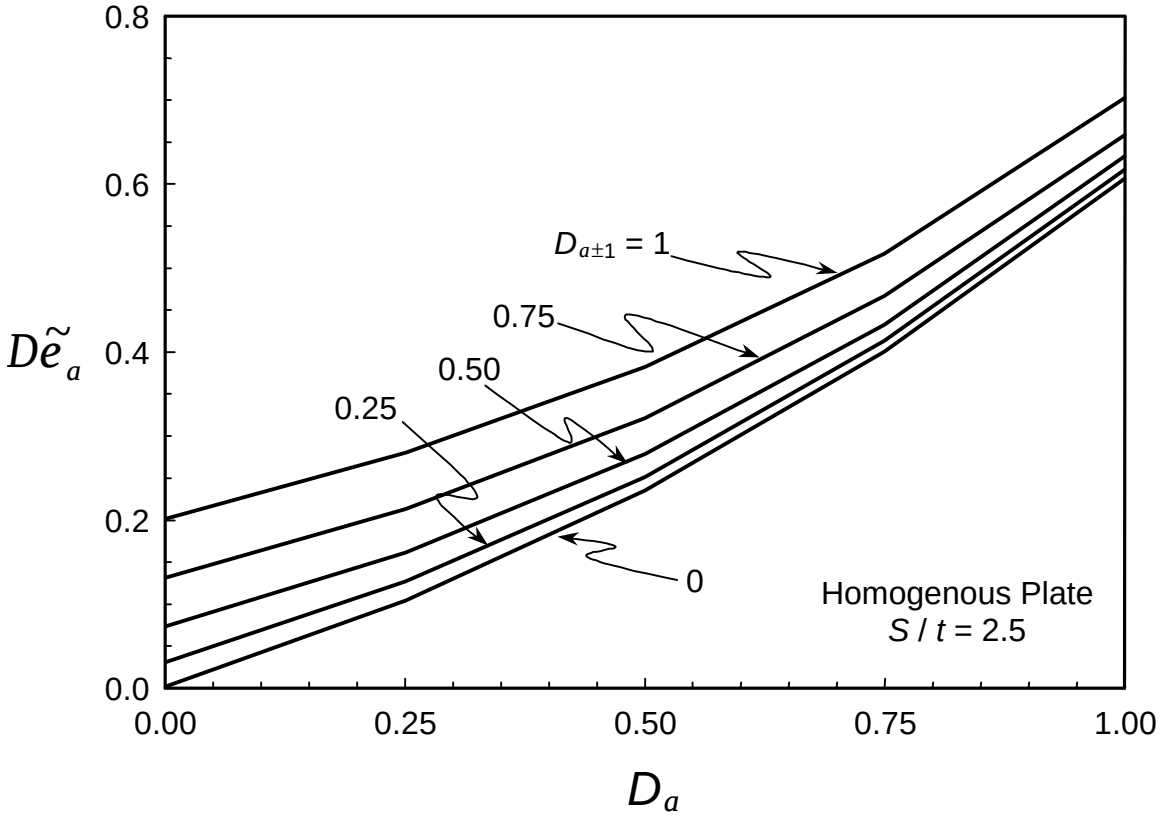

Fig. 10. Effect of damage on strain measurement in sector a is shown for different combinations of D_a and $D_{a\pm1}$ (homogeneous plate with S / t = 2.5).

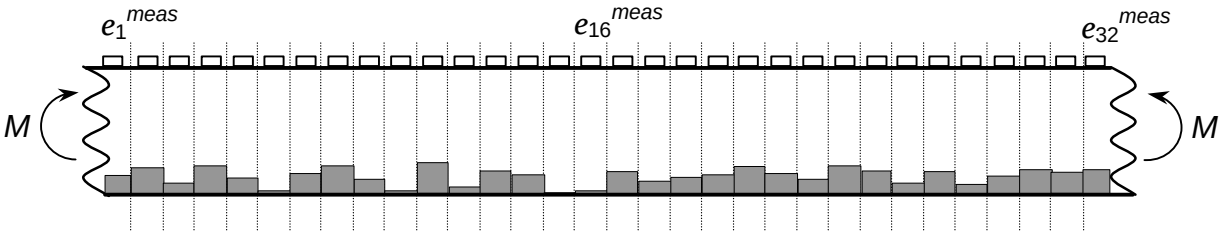

(a)

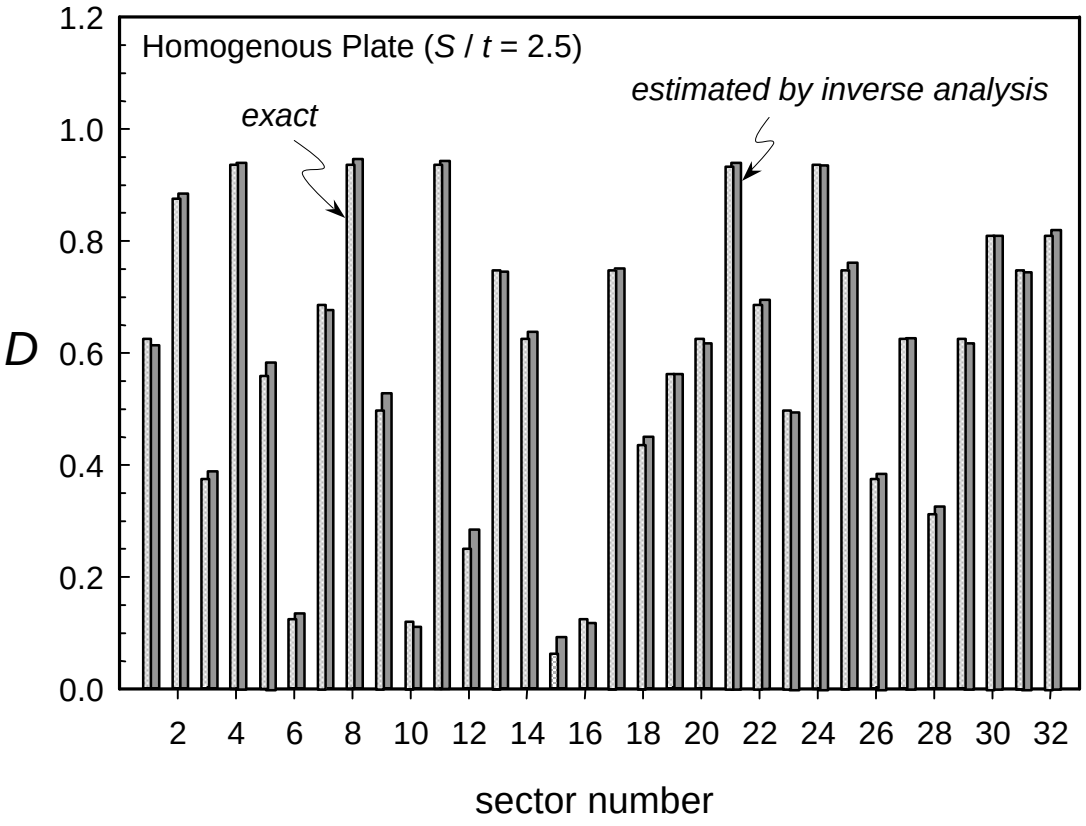

(b)

Fig. 11. (a) Homogenous plate subjected to bending with randomly varied damage in different sectors (constant within a sector) for smaller sector width (S / t = 2.5). Vertical dimensions are magnified by 10 times. (b) Distributions of exact/prescribed damage and estimated damage across sectors.

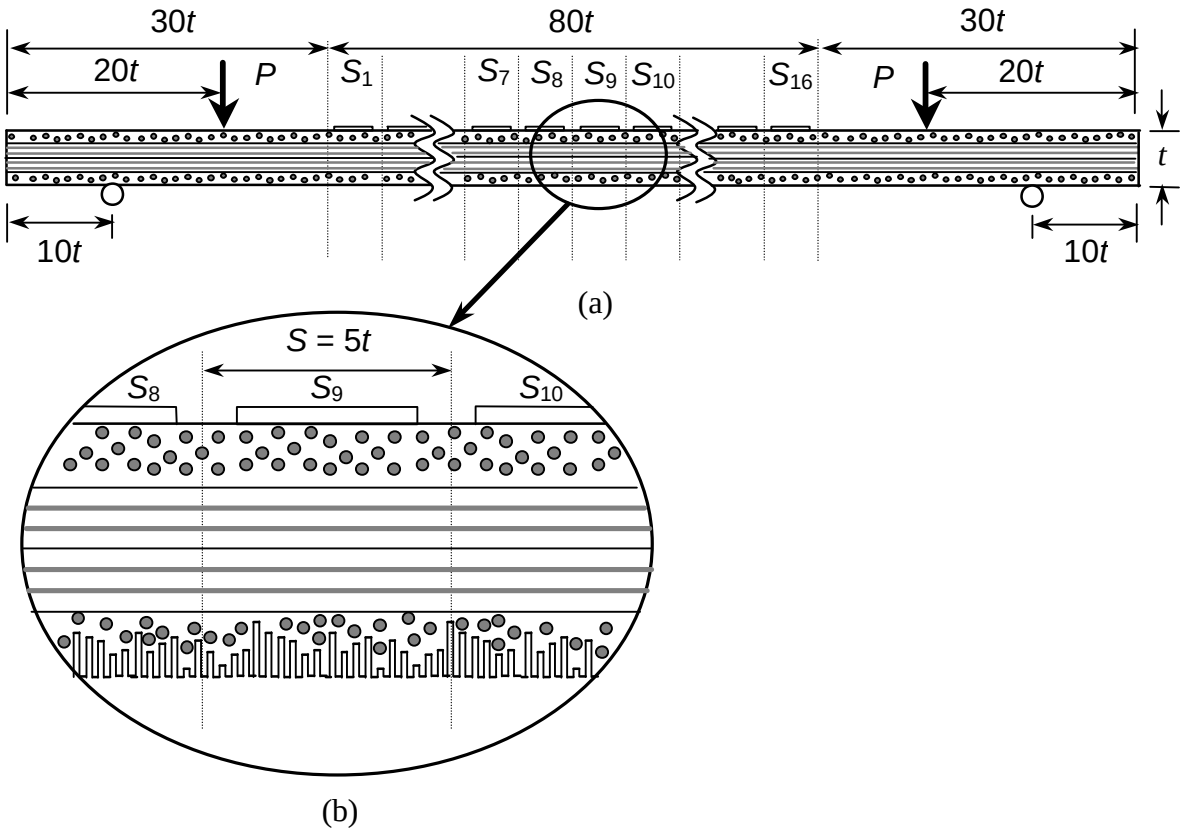

Fig. 12. (a) Surface damaged 4-ply $[90/0]_s$ composite laminate subjected to four-point-bend. (b) Enlarged section of model showing comb-like degradation on exposed surface. Vertical dimensions are magnified by 5 times for clarity.

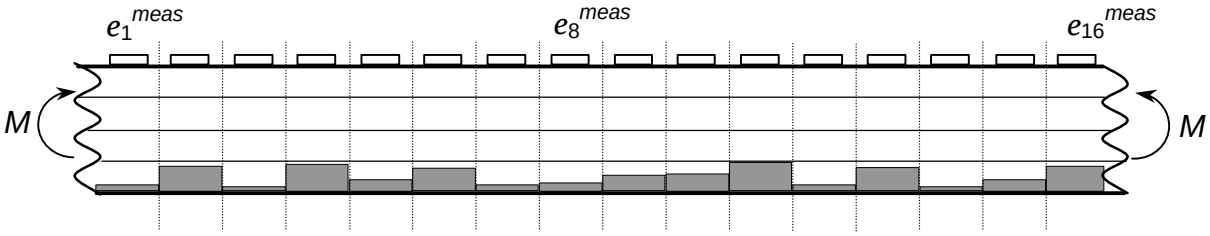

(a)

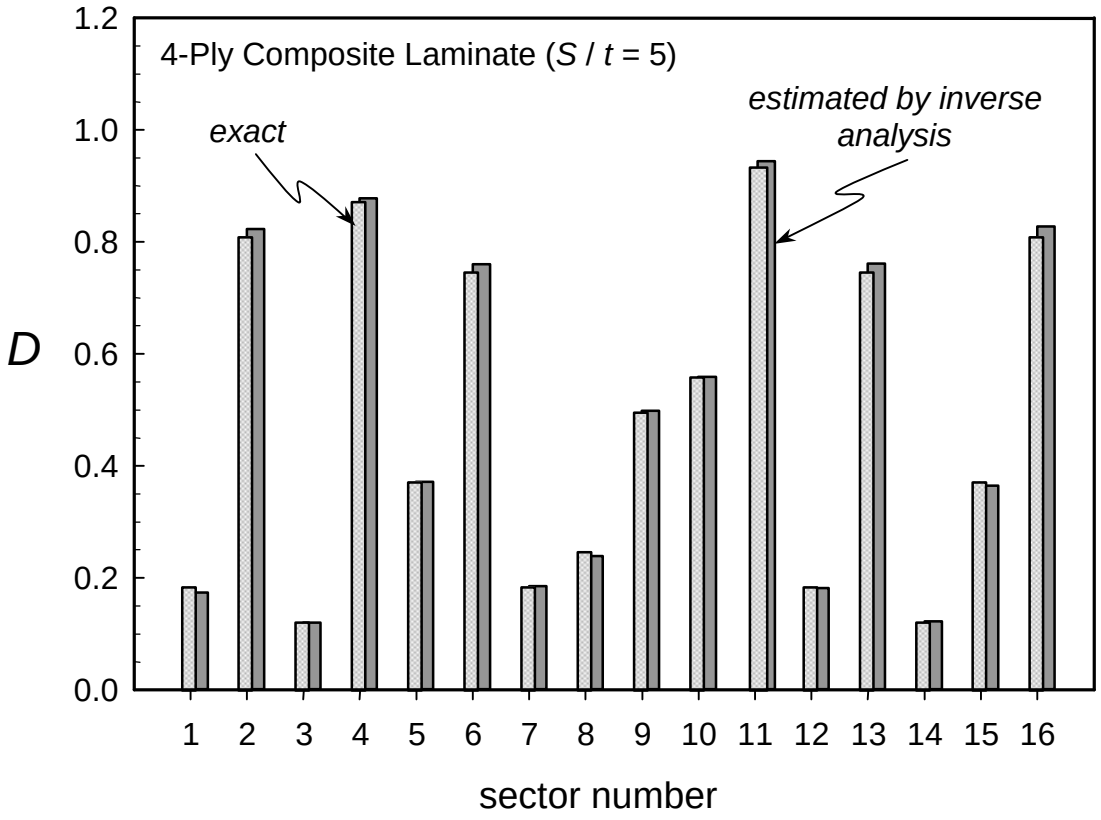

(b)

Fig. 13. (a) 4-ply composite laminate subjected to bending with randomly varied damage in different sectors (constant within a sector). Vertical dimensions are magnified by 10 times. (b) Distributions of exact/prescribed damage and estimated damage across sectors.

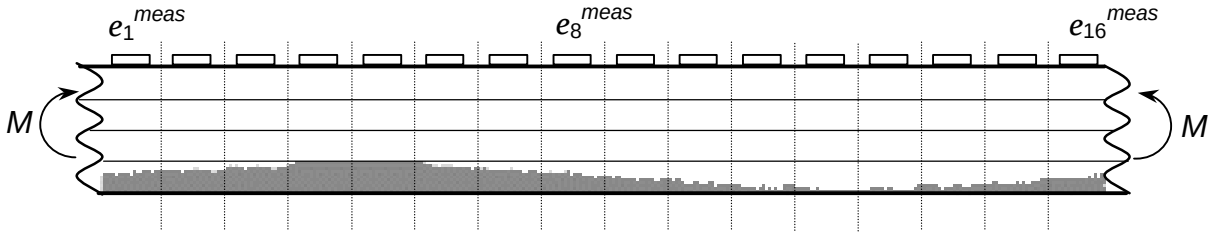

(a)

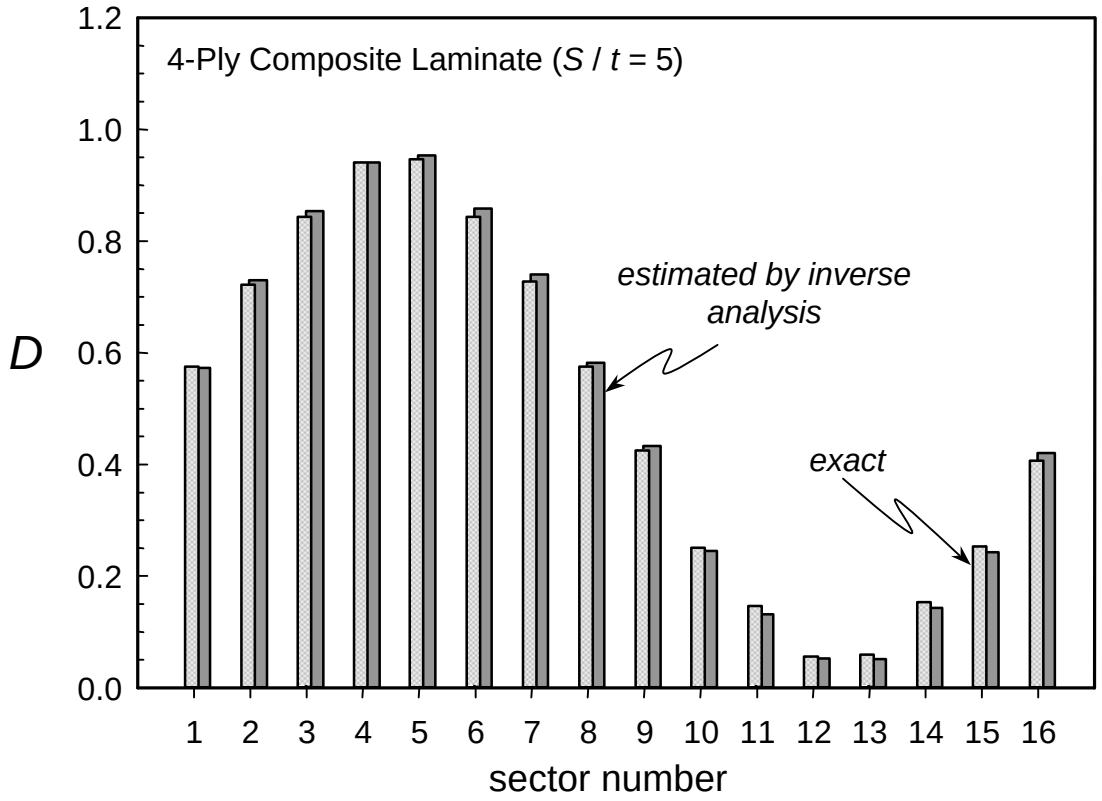

(b)

Fig. 14. (a) 4-ply composite laminate subjected to bending with sinusoidal damage distribution. In each sector, magnitudes are varied randomly within small range. Vertical dimensions are magnified by 10 times. (b) Distributions of exact/prescribed damage and estimated damage across sectors. Damages within each sector are averaged.

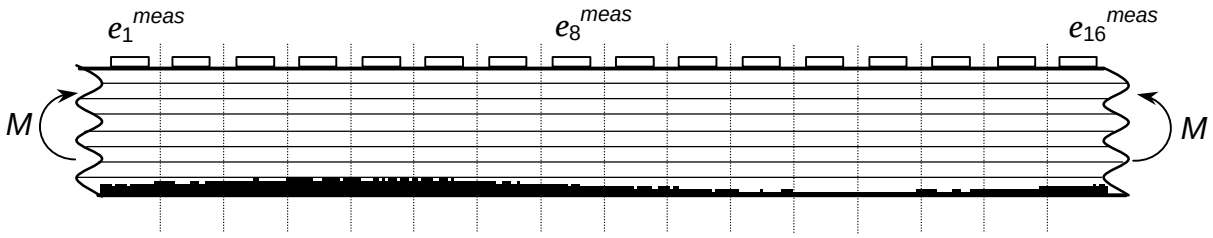

(a)

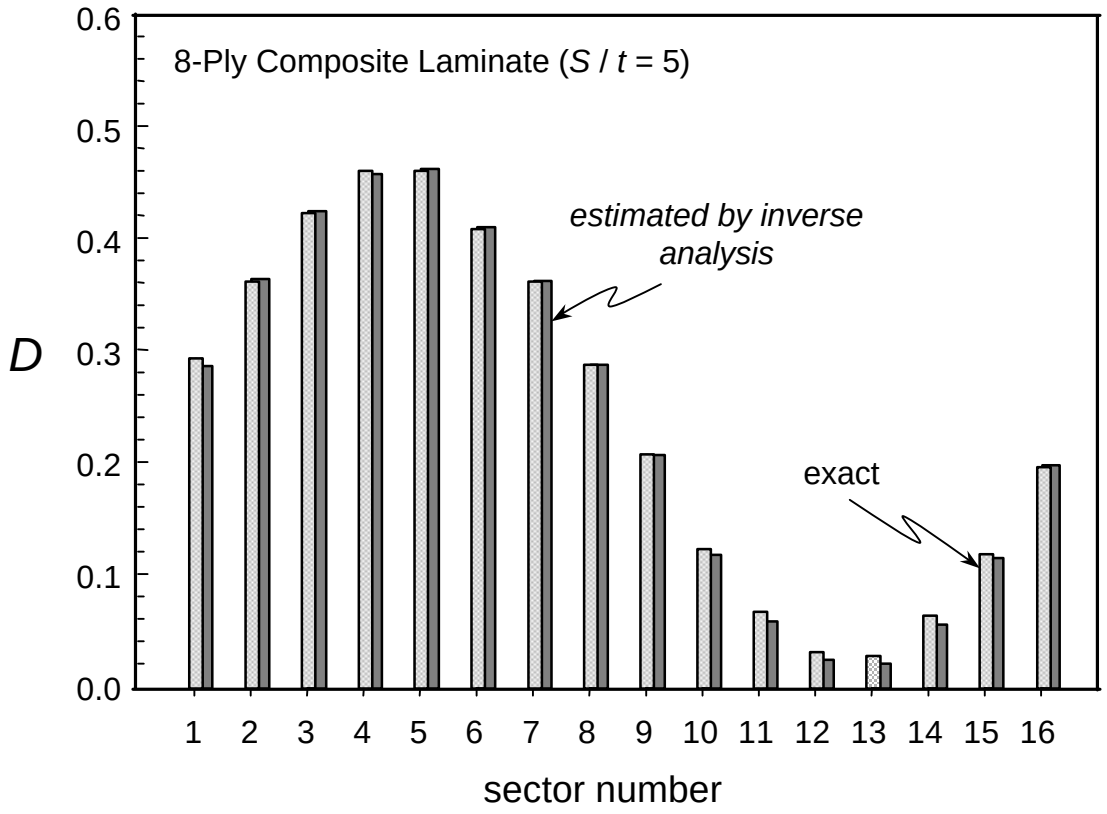

(b)

Fig. 15. (a) 8-ply composite laminate subjected to bending with sinusoidal damage distribution. In each sector, magnitudes are varied randomly within small range. Vertical dimensions are magnified by 10 times. (b) Distributions of exact/prescribed damage and estimated damage across sectors. Damages within each sector are averaged.